Journal of Helminthology

www.cambridge.org/jhl

Auranofin attenuates *Schistosoma mansoni* egg-induced liver granuloma and fibrosis in mice

A.F. Atia[1], N.M. Abou-Hussien[1], D.M. Sweed[2], E. Sweed[3] and N.A. Abo-khalil[1]

[1]Medical Parasitology Department, Faculty of Medicine, Menoufia University, Shebin El-Kom, Menoufia, Egypt; [2]Pathology Department, National Liver Institute, Menoufia University, Shebin El-Kom, Menoufia, Egypt and [3]Clinical Pharmacology Department, Faculty of Medicine, Menoufia University, Shebin El-Kom, Menoufia, Egypt

Research Paper

Cite this article: Atia AF, Abou-Hussien NM, Sweed DM, Sweed E and Abo-khalil NA (2023). Auranofin attenuates *Schistosoma mansoni* egg-induced liver granuloma and fibrosis in mice. *Journal of Helminthology*, **97**, e95, 1–10
https://doi.org/10.1017/S0022149X23000792

Received: 07 September 2023
Revised: 09 November 2023
Accepted: 09 November 2023

Keywords:
Auranofin; liver granuloma; *Schistosoma mansoni*; NLRP3; SIRT3

Corresponding author:
E. Sweed;
Email: eman.sweed@med.menofia.edu.eg

Abstract

Schistosomiasis is a serious tropical disease. Despite extensive research into the etiology of liver fibrosis, effective therapeutic options remain limited. This study aims to assess the effectiveness of auranofin in treating hepatic granuloma and fibrogenesis produced by *Schistosoma (S.) mansoni* eggs. Auranofin is a gold complex that contains thioglucose tetraacetate and triethylphosphine. Eighty BALB/c male mice were divided into four groups (n=20/group): negative control (GI), positive control (GII), and early (GIII) and late (GIV) treatment groups with oral auranofin according to beginning of treatment 4th week and 6th week post-infection. Mice were infected subcutaneously in a dose of 60±10 cercariae/mouse. Worm counts, egg loads, and oogram patterns were determined. Biochemical, histological, and immunostaining of interleukin-1β (IL-1β), Sirtuin 3 (SIRT3), and smooth muscle actin (SMA) were assessed. GIII showed a significant decrease in the total *S. mansoni* worm burden and ova/gram in liver tissue (with reduction percent of 63.07% and 78.26%, respectively). Schistosomal oogram patterns, immature and mature ova, also showed a significant decrease. The reduction in granuloma number and size was 40.63% and 48.66%, respectively, in GIII, whereas in GIV, the reduction percent was 76.63% and 67.08%. In addition, the degree of fibrosis was significantly diminished in both treated groups. GIV showed significant reduction in IL-1β and SMA expression and increase in SIRT3 expression. These findings reveal how auranofin suppresses the development of liver fibrosis. Therefore, it is crucial to take another look at auranofin as a prospective medication for the treatment of *S. mansoni* egg-induced hepatic granuloma and consequent fibrosis.

Introduction

A helminthic infectious disease, schistosomiasis affects 240 million people worldwide and has spread to 74 nations and regions. It is most common in tropical and sub-tropical areas (WHO 2022). After the eggs mechanically occlude the microvasculature, early pathological alterations appear, leading to acute vasculitis with endothelial injury and necrosis (Van de Vijver *et al.* 2006). Following the enrollment of immunological and inflammatory cells at infection areas because of the lodged ova's sustained antigenic stimulation, some infected people develop chronic fibrosis and granulomas (Chuah *et al.* 2014). For liver fibrosis in schistosomiasis, activation of hepatic stellate cells is essential (Zhang *et al.* 2019). Interleukin-1β (IL-1β), tumor necrosis factor (TNF), and transforming growth factor (TGF) are a few examples of inflammatory cytokines or chemokines that Kupffer cells (KCs) can swiftly release in response to hepatic damage (Wree *et al.* 2014). These elements may promote hepatic stellate cell (HSC) activation and proliferation, which may lead to the production of extracellular matrix (ECM), and so cause liver fibrosis (Wree *et al.* 2018).

Nucleotide-binding oligomerization domain-like (NOD-like) receptors are intracellular sensors of pathogen-associated molecular patterns that are linked to cell stress and damage-associated chemical patterns that enter the cell by phagocytosis or holes. They are important players in the control of the innate immune response (Mahla *et al.* 2013). Toll-like receptors and NOD-like receptors can work together to regulate inflammatory and apoptotic responses (Franchi *et al.* 2009). Complex protein NOD-like receptor protein 3 (NLRP3) is primarily produced in macrophages and is a part of the inflammasome that recognizes by-products of injured cells (Lu and Wu 2015). Caspase-1 activation can encourage the generation of IL-1β and IL-18 and protect against certain pathogen damage (Cao *et al.* 2019). In situations including Angiotensin II, steatohepatitis induced by alcohol, and drug-induced liver damage, there is growing evidence connecting the inflammation caused by the NLRP3 inflammasome leading to tissue damage and liver fibrosis (Nagy 2015; Ning *et al.* 2017). According to earlier research, the NLRP3 inflammasome regulates macrophage and HSC activity, which is essential for the advancement of fibrosis (Inzaugarat *et al.* 2019; Wree *et al.* 2018; Zhang *et al.* 2019).

New therapeutic drugs for treating hepatic fibrosis offer a promising target in the inhibition of the NLRP3 inflammasome.

Autophagy is a cellular mechanism that has been conserved throughout evolution and is crucial for the survival and upkeep of cells by destroying organelles, proteins, and macromolecules (Ding *et al.* 2021). Pro-IL-1β, mitochondria, and the inflammasome components are all degraded by autophagosomes, which reduces IL-1β release (Levine and Deretic 2007). In response to metabolic or extrinsic stress, NLRP3 inflammasome activation was enhanced in macrophages with impaired autophagy (Lee *et al.* 2016).

There are seven sirtuins (SIRT1 to 7) in mammalian cells. Sirtuins are a class of nicotinamide adenine dinucleotide+ (NAD +) dependent deacetylases. Sirtuin 3 (SIRT3) is largely located in mitochondria as the major regulator of mitochondrial protein acetylation (Xu *et al.* 2016). SIRT3 is a key regulator of mitochondrial functions that control energy production, metabolism, and the body's reaction to oxidative stress. It is highly expressed in tissues with a high rate of metabolic activity, including the liver (Hirschey *et al.* 2010). Additionally, SIRT3-induced autophagy suppressed NLRP3 inflammasome activation in macrophages (Liu *et al.* 2018).

Although chemotherapy successfully eradicates adult worms and inhibits the accumulation of schistosome eggs, less effective medications are focused on treating hepatic fibrosis that has already developed, particularly in the chronic and severe phases of the illness. In recent years, significant efforts have been made to find medications that target hepatic fibrosis in schistosomiasis (Niu *et al.* 2022).

As an anti-rheumatic medication, auranofin has been used in therapeutic settings. It stops osteoclast differentiation by inhibiting the NLRP3 inflammasome. (Kuntz *et al.* 2007). Additionally, the mechanism by which auranofin inhibits schistosomiasis has been thoroughly studied (Angelucci *et al.* 2009). It was found that auranofin reduced worm burden in *S. mansoni*-infected mice likely through inhibition of Thioredoxin glutathione reductase (TGR) (Kuntz *et al.* 2007), and it has in vitro worm-killing action (Kim *et al.* 2019). Two experimental liver fibrosis models were used to evaluate the possibility of using auranofin clinically to treat liver fibrosis (Kim *et al.* 2021); however, the liver fibrosis caused by *S. mansoni* differs from other models of liver fibrosis in that the host is impacted by the stimulation of the eggs and the growth of the worm. Therefore, we hypothesized that auranofin's anti-inflammatory effects, activating macrophage autophagy and preventing inflammasome activation, will alleviate *S. mansoni* egg-induced liver granuloma and later development of hepatic fibrosis.

Material and methods

Animals

Eighty male BALB/c laboratory-bred mice were purchased from Theodor Bilharz Research Institute (TBRI), Imbaba, Giza, Egypt. They were eight weeks old, weighed 18–20 grams, and were parasite-free. After receiving the approval of the National Liver Institute's Ethical Committee (IRB00383/2022), they were maintained at 27±2°C. They were kept to a standard diet and water ad libitum. The cages were cleaned twice a week to ensure good sanitary conditions. This was done in compliance with the ARRIVE guidelines (Percie du Sert *et al.* 2020).

Cercariae

Cercariae of a virulent strain of *S. mansoni* were isolated from infected *Biomphelaria alexandrina* snails raised and maintained at TBRI. The *S. mansoni cercariae* were isolated by the procedure described in Liang *et al.* (1987), and the removed cercariae were counted by a stereomicroscope (Mohamed *et al.* 2011). Mice were infected subcutaneously in a dose of 60±10 cercariae/mouse using the technique in Holanda *et al.* (1974).

Drug and dose

Auranofin® was provided by Tocris Bioscience (a Bio-Techne Brand, Minneapolis, Minnesota, USA) and was dissolved in 100% ethanol. A dose of auranofin that is safe for healthy mice was given orally at a dose of 1 mg/kg twice daily for nine days (Andrade *et al.* 2014; Debnath *et al.* 2013).

Experimental design

The mice were divided into four groups each consisting of 20 mice. (1) Negative control group (Group I/GI); non-infected non-treated mice which were subdivided equally into two subgroups (GIa and GIb) each including 10 mice. (2) Positive control group (Group II/GII); infected non-treated mice which were subdivided equally into two subgroups (GIIa and GIIb) each including 10 mice. (3) Early treated group (Group III/GIII) infected mice were treated orally by gastric gavage with auranofin (1 mg/kg twice daily for 9 days), starting on the 4th week post-infection (p.i.). (4) Late-treated group (Group IV/GIV) infected mice were treated orally by gastric gavage with auranofin (1 mg/kg twice daily for 9 days) beginning the 6th week p.i. (This helps in analyzing auranofin's impact on S. mansoni egg-induced liver fibrosis) (Table 1).

Sacrifice and perfusion

Mice from groups GIa, GIIa, and GIII were sacrificed on the 6th week p.i. (anesthetized with ether and euthanized by decapitation) to assess the effect of auranofin on *S. mansoni* egg-induced liver granuloma. From each mouse, portions of the liver were taken after the worm count to determine the egg burden and oogram pattern. For histopathological studies, liver samples were collected. Sera were isolated from blood samples and used for biochemical investigations. To determine how auranofin affects *S. mansoni*-induced

Table 1. Experimental groups

Groups	Early-treated	Late-treated	Total number of mice (80)
Negative control	GIa (N=10)	GIb (N=10)	20
Positive control	GIIa (N=10)	GIIb (N=10)	20
Treated groups	GIII (N=20)	GIV (N=20)	40

The mice were divided into four groups, each consisting of 20 mice.
(1) Negative control group (Group I/GI): non-infected, non-treated mice which were subdivided equally into two subgroups (GIa and GIb), each including 10 mice.
(2) Positive control group (Group II/GII): infected, non-treated mice which were subdivided equally into two subgroups (GIIa and GIIb), each including 10 mice.
(3) Early-treated group (Group III/GIII): infected mice were treated orally by gastric gavage with auranofin (1 mg/kg twice daily for 9 days), starting on the 4th week post-infection (p.i.).
(4) Late-treated group (Group IV/GIV): infected mice were treated orally by gastric gavage with auranofin (1 mg/kg twice daily for 9 days), beginning the 6th week p.i. (This helps in analyzing auranofin's impact on *S. mansoni* egg-induced liver fibrosis).
N: number per group

https://doi.org/10.1017/S0022149X23000792 Published online by Cambridge University Press

liver fibrosis; mice of the GIb, GIIb, and GIV groups were sacrificed on the 10th week p.i., and liver samples were collected for histopathological and immunohistochemical studies. As with the early-treated group, blood samples were also collected, and sera were divided for biochemical investigations.

Parasitological studies

Porto-mesenteric worm burden and reduction %

S. mansoni adult worms (males, females, and couples) that emerged from the portomesenteric system following perfusion were counted. The percentage reduction of adult worms after treatment was calculated according to Tendler *et al.* (1986) using the formula R = C−V/C × 100, where R = reduction %, C = mean number of adult worms from infected non-treated mice, and V = mean number of parasites from treated mice.

Tissue egg load/g intestine and liver

The livers of sacrificed infected mice were weighed and then digested in 5% KOH solution. The number of eggs per gram of liver was calculated under a light microscope at 40× magnification (Cheever 1969).

Oogram pattern

Three fragments from the ileum of each mouse (1 cm each) were cut longitudinally, rinsed with saline, and dried gently using Whatman filter paper. They were examined microscopically, and the percentage of different egg developmental stages (oogram pattern) was studied using the technique of Pellegrino *et al.* (1962), which involved identifying and counting eggs at various stages of maturity.

Histopathological studies

Specimens from the liver tissue of mice infected with *S. mansoni* and treated with auranofin were obtained. The specimens were preserved in 10% neutral buffered formalin (pH 7.2), embedded in paraffin blocks, and sliced at a thickness of 4–5 µm. The tissue sections from all groups were stained according to Bancroft and Gamble (2008). The histopathological characteristics were evaluated using standard H&E to determine the number and measure the diameter of *Schistosoma* granulomas using twenty non-overlapping high-power fields (400X). Eosinophils per granuloma region were also counted. Moreover, types of granulomas were assessed and divided into four major evolutionary stages: (1) pre-granulomatous exudative, characterized by an infiltrate of inflammatory cells in the process of organization around the parasite egg; (2) necrotic-exudative, distinguished by a central halo of necrosis and numerous inflammatory cells dispersed irregularly on subsequent layers; (3) exudative-productive, distinguished by a rich structure of collagen fibers and inflammatory cells concentrated in the periphery and exhibiting a more organized and circumferential aspect; and (4) productive, with a characteristic thick band of collagen fibers separating the egg from a small number of inflammatory cells. The total area connected to the granulomatous reaction was used to calculate the size of granulomas using semi-automated methods (Amaral *et al.* 2017). In addition, Masson trichome (MT) stain was done to assess collagen deposition in the liver tissue of groups GIIb and GIV. Briefly, slides were stained for 10 minutes with Weigert's iron hematoxylin working solution, washed, stained for 15 minutes with Biebrich scarlet-acid fuchsin solution, washed, immersed for 15 minutes in phosphomolybdic-phosphotungstic acid solution, transferred directly to aniline blue solution for 10 minutes, quickly washed in distilled water, and then transferred to 1% acetic acid solution for 5 minutes. Collagen strands were stained blue, while hepatocytes were stained red. Microscopy and photo taking were carried out using an Olympus CX41 microscope and a DP26 camera in Shinjuku, Tokyo, Japan.

Immunohistochemical (IHC) studies

The streptavidin-biotin system was used for the immunostaining procedure. Interleukin-1β (IL-1β) diluted to 1:50 (Cat. #12242), Sirtuin 3 (SIRT3) diluted to 1:200 (Cat. #2627), and smooth muscle actin (SMA) diluted to 1:400 (Cat. #19245) were obtained from Cell Signaling Technology, Massachusetts, USA. Before antigen retrieval, the tissue was deparaffinized and rehydrated in a high pH ethylenediaminetetraacetic acid (EDTA) solution for 20 minutes. After that, it was cooled at room temperature for an additional 20 minutes. The primary antibodies were applied to each plate and left overnight at 4°C. Horseradish peroxidase/3,3'-diaminobenzidine (HRP/DAB) secondary antibody, ready for applying Mayer's hematoxylin as a counterstain and DAB chromogen substrate to visualize the staining, SIRT3, IL-1β, and SMA markers were employed. In every test, both positive and negative controls were used. SMA and IL-1β antibodies exhibited cytoplasmic localization, whereas SIRT3 antibody showed nuclear and cytoplasmic localization. Histoscore (H score) was used to evaluate expression. The intensity and percentage of cells were multiplied as follows: (strong intensity (3) x percentage) + (moderate intensity (2) x percentage) + (mild intensity (1) x percentage) + (negative staining (0) x percentage). A final score between 0 and 300 was established (Pu *et al.* 2017).

Assessment of liver function

Serum samples were separated by centrifugation at 3000 rpm for ten minutes. Liver function tests for alanine transaminase (ALT) and aspartate transaminase (AST) were performed using an Integra 400 autoanalyzer (Roche, Germany). Quantitative determination of AST and ALT was carried out by the Warburg method with pyridoxal-5-phosphate at a wavelength of 340 nm according to the International Federation of Clinical Chemistry (IFCC) protocol (Bergmeyer *et al.* 1986).

Statistical analysis

Data were collected, tabulated, and analyzed by Statistical Package of Social Science (SPSS) version 22 (Armonk, NY: IBM Corp, 2013) and GraphPad Prism version 8.0.0 for Windows (GraphPad Software, San Diego, California, USA). The mean (X) and standard deviation (SD) were used to present quantitative data, and the T test was used to compare data between two groups. Numbers and percentages were used to show qualitative data. To compare qualitative variables, the Monto-Carlo test was used. Statistics were considered significant at P values ≤ 0.05.

Results

The overall *S. mansoni* worm burden and ova gram/liver tissue were significantly decreased (63.07% and 78.26%, respectively, $P < 0.001$) in GIII when compared to the infected control group (GIIb), whereas in GIV, the decrease was 56.08% and 69.67%, respectively

https://doi.org/10.1017/S0022149X23000792 Published online by Cambridge University Press

Table 2. Comparison of mean *S. mansoni* worm burdens and egg load studied groups

Groups Parameters	Early phase				Late phase			
	GIIa	GIII	% reduction	P value	GIIb	GIV	% reduction	P value
No of ♂	6.80 ± 1.49	2.30 ± 0.36	66.17 %	P < 0.001	7.50 ± 1.57	3.20 ± 0.24	57.33%	P < 0.001
Number of_♀	4.80 ± 1.20	2.00 ± 0.47	58.33%	P < 0.001	5.70 ± 1.40	2.90 ± 0.35	49.12%	P < 0.001
Number of couples ♂♀	31.00 ± 2.75	11.90 ± 1.39	61.61%	P < 0.001	42.20 ± 3.12	20.40 ± 2.1	51.56%	P < 0.001
Total worm load	43.60 ± 3.25	16.10 ± 1.23	63.07%	P < 0.001	52.60 ± 2.55	23.10 ± 1.89	56.08%	P < 0.001
Ova gram tissue liver	10400.00 ± 1194.57	2260.00 ± 172.69	78.26%	P < 0.001	12200.00 ± 1232.52	3700 ± 184.62	69.67%	P < 0.001

T test was used. Values are expressed as mean ± standard deviation. GIIa: early positive control group (n=10); GIII: early-treated group infected mice with auranofin (n=20), ♂: male, ♀: female; GIIb: late positive control group (n=10); GIV: late-treated group infected mice with auranofin (n=20), ♂: male, ♀: female

Table 3. Comparison of oogram patterns in studied groups

Groups Parameters	Early phase			Late phase		
	GIIa	GIII		GIIb	GIV	
	Mean ± SD	Mean ± SD	P value	Mean ± SD	Mean ± SD	P value
Immature egg	55.20 ± 2.20	26.80 ± 1.25	P < 0.001	56.10 ± 1.40	29.70 ± 1.44	P < 0.001
Mature egg	43.40 ± 1.50	20.40 ± 0.872	P < 0.001	42.20 ± 1.20	24.24 ± 0.65	P < 0.001
Oogram dead egg	4.20 ± 0.86	38.70 ± 1.44	P < 0.001	4.60 ± 0.44	40.50 ± 1.69	P < 0.001

T test was used. Values are expressed as mean ± standard deviation. GIIa: early positive control group (n=10); GIII: early-treated group infected mice with auranofin (n=20); GIIb: late positive control group (n=10); GIV: late-treated group infected mice with auranofin (n=20)

(Table 2). Regarding the schistosomal oogram pattern, there was a statistically significant difference between the means of immature eggs and mature ova (26.80 ± 1.25 and 20.40 ± 0.872, respectively, P < 0.001) in the early-treated group (GIII) and the control infected group (GIIa), which were (55.20 ± 2.20 and 43.40 ± 1.50, respectively, P < 0.001). In addition, there was a significant difference between the two groups regarding the mean number of dead eggs, which was 38.70 ± 1.44 in the GIII group against 4.20 ± 0.86 in the control-infected group (P < 0.001). Meanwhile, in GIV, the means of immature eggs and mature ova were 29.70 ± 1.44 and 24.24 ± 0.65, respectively, and the mean number of dead eggs was 40.50 ± 1.69 with a statistically significant difference with GIIb (P < 0.001) (Table 3).

Histopathological results

There was a high density of hepatic granuloma and a significantly larger area of eosinophil-rich granuloma in the infected control subgroups (GIIa and GIIb) (Figure 1a and d and Table 4). While in the early-treated GIII, the reduction percent in granuloma number and size was 40.63% (P < 0.001) and 48.66% (P = 0.108), respectively, with a predominant exudative/necrotic granuloma type and reduced eosinophilic count (Figure 1b and e and Table 4). Meanwhile, the best reduction in granuloma number and size was 76.63% (P < 0.001) and 67.08% (P = 0.008), respectively, in GIV (the late-treated group) (Table 4), and the form of granuloma was productive, with a low eosinophil count (Figure 1c and f). The infected and treated groups both had *Schistosoma* granulomas at various phases of development.

Collagen deposition in the liver tissue assessed by MT stain was significantly decreased in the GIV (late-treated group) as compared to the GIIb (infected control) that showed marked periportal fibrosis (Figure 1g, h, and j and Table 4).

When compared to the infected groups, the density of hepatic granulomas and the eosinophilic-rich infiltrate were significantly lower in both treated groups (P < 0.001) (Table 4). In GIV, the granulomas were significantly smaller than those in the late-infected group (P = 0.008). In addition, the degree of fibrosis was significantly decreased (P = 0.025) (Table 4).

Immunohistochemical results

Interleukin-1β expression was significantly reduced in the GIII and GIV, with GIV significantly exhibiting the lowest expression (P < 0.001), whereas the infected control groups (GIIa and GIIb) had significantly higher levels of IL-1β (H score was 82.00 ± 4.89 and 94.00 ± 2.44, respectively) (Table 5 and Figure 2a, b, and c). However, SIRT3 expression was low in GIIa and GIIb (H score was 14.00 ± 2.91 and 13.00 ± 4.35, respectively). SIRT3 expression was significantly higher in both treated groups compared to the infected, with the highest expression observed in GIV (late-treated) (H score was 224.00 ± 5.61) (P < 0.001) (Table 5 and Figure 2d, e, and f). The liver tissue of GIIa and GIIb revealed significant SMA expression in both portal tracts and sinusoidal HSC (H score was 69.00 ± 2.00 and 83 ± 3.00, respectively). Smooth muscle actin expression was highly significantly reduced in GIV (H score was 10.50 ± 1.38) (P < 0.001) (Table 5 and Figure 2g, h, and j).

Results of ALT and AST serum levels

The serum levels of ALT and AST were improved in both treated groups, GIII (31.76 ± 0.30 and 45.73 ± 0.76) and GIV (28.25 ± 0.36 and 39.22 ± 0.31), respectively (P < 0.05), when compared to the infected control group, with a significant difference, GIIa (65.88 ± 0.32 and 76.88 ± 0.68) and GIIb (79.02 ± 0.52 and 89.28 ± 0.41), respectively (P < 0.05). Additionally, there was a notable difference between the two treated groups, GIII and GIV (Figure 3).

https://doi.org/10.1017/S0022149X23000792 Published online by Cambridge University Press

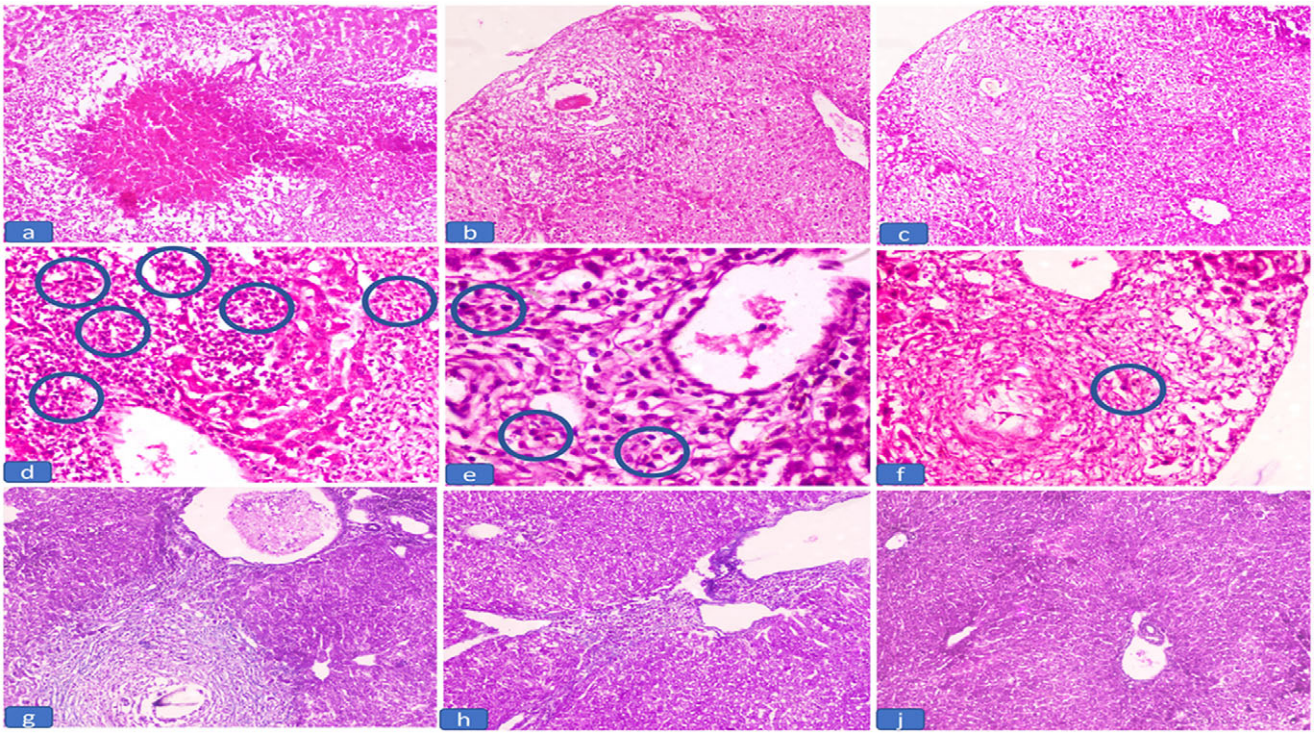

Figure 1. The histopathological findings of liver tissue in the studied groups. a) Exudative necrotic granuloma in infected untreated groups (GIIa and GIIb) (H&E, 100x), b) Exudative granuloma in early-treated group (GIII) (H&E, 100x), c) Productive granuloma in the late-treated group (GIV) (H&E, 100x), d) Dense eosinophilic count in the inflammatory infiltrate in the infected untreated groups (GIIa and GIIb) (circles) (H&E, 400x), e) Decrease eosinophilic count in the inflammatory in the early-treated groups (GIII) (circles) (H&E, 200x), f) Few eosinophilic count in the inflammatory in the late-treated groups (GIV) (circles) (H&E, 200x), g) Marked periportal fibrosis in infected untreated group (GIIb) (MT, 100x), h) Mild periportal fibrosis in the late-treated group (GIV) (MT, 100x), j) No periportal fibrosis in the late-treated group (GIV) (MT, 100x).

Discussion

The most severe pathological manifestations of schistosomiasis are hepatic granulomas and fibrosis, which are caused by egg deposition in the liver (Zhang *et al.* 2019). The development of hepatic fibrosis is heavily influenced by chronic inflammation and the activation of inflammasomes (Alegre *et al.* 2017). Auranofin is clinically approved for the treatment of rheumatoid arthritis, and it has lately been researched for potential therapeutic uses in a variety of illnesses (Chen *et al.* 2022; Steers *et al.* 2022). In this work, we examined the impact of auranofin on liver granuloma and fibrosis caused by *S. mansoni* eggs.

The administration of auranofin to infected mice resulted in a significant decrease in the total worm burden and tissue egg load with an increase in the degenerating ova, contrary to the infected control group. Auranofin decreased worm burden in mice with *S. mansoni* infection, probably via inhibiting TGR (Kuntz *et al.* 2007).

Regarding the histopathological results, when compared to the control groups, auranofin considerably reduced the mean hepatic granuloma diameter and number in both early and late treatment groups ($P < 0.001$), with a predominance of degraded ova. Masson's trichrome staining showed that auranofin reduced fibrosis and significantly improved gross hepatic morphology with a lower percentage of collagen in the late-treated group. Since there are no first-line treatments for liver fibrosis, a study's findings demonstrate auranofin therapeutic efficacy in liver fibrosis (Kim *et al.* 2021).

In this study, the *S. mansoni*-infected group had significantly higher serum levels of ALT and AST, which indicated liver damage, as previously reported by El-Refai *et al.* (2019). Administration of auranofin significantly improved their levels in both treated groups. Similar results were reported by Kim *et al.* (2023) who stated that mice treated with auracyanide had normal serum levels of AST and ALT, indicating that auracyanide, an active metabolite of auranofin, may prevent liver fibrosis.

NLRP3 inflammasome has been the focus of some of the most recent research to date regarding its effects on numerous human diseases, antiviral responses, and antifungal responses (He *et al.* 2018; Lee *et al.* 2013; Mao *et al.* 2014; Vakrakou *et al.* 2018). Additionally, it can be found in the cytoplasm of HSCs and can be triggered by several different pathogens, including *S. mansoni*, *E. coli*, and *S. japonicum* (Chen *et al.* 2019; Meng *et al.* 2016). The activation of caspase-1 and the subsequent release of IL-1β are made possible by the NLRP3 inflammasome, which is crucial in the development of hepatic fibrosis and inflammation (Kaufmann *et al.* 2022). In addition, collagen deposition and NLRP3 activation in primary human hepatocytes results in pyroptotic cell death (Gaul *et al.* 2021). The adaptive innate immune responses to the development of fibrosis are controlled by the NLRP3 inflammasome. In liver fibrosis, IL-1β and TNF-α promote interactions between immune cells and HSCs (Seki and Schwabe 2015).

We examined auranofin's impact on the release of IL-1β to clarify how it affects the NLRP3 inflammasome's activation. This study demonstrated that auranofin therapy decreased IL-1β expression in the GIII (early) and GIV (late) treated groups, with GIV significantly exhibiting the lowest expression. It demonstrates that auranofin limits the synthesis of inflammatory cytokines and inhibits innate immune signaling by acting on numerous domains. Similarly, Zhang *et al.* (2012) discovered that hepatocyte necrosis

https://doi.org/10.1017/S0022149X23000792 Published online by Cambridge University Press

Table 4. The comparison between different groups regarding the pathological data

	Normal	Early phase			Chronic phase		
	I	IIa	GIII	P value	IIb	GIV	P value
No of hepatic granuloma (20 HPF)	0	21.8 ± 2.1	13 ± 0.9	P1 = 0.000	24.4 ± 1	5.7 ± 0.2	P2 = 0.000
P = 0.000, between III and IV							
Size of hepatic granuloma (10 HPF)	0	8698 ± 1186.8	4464.7 ± 502.2	P1 = 0.108	8898 ± 1313	2929.1 ± 1489.6	P2 = 0.008
P = 0.840, between III and IV							
No. of eosinophils (40 HPF)	0	320 ± 25.5	48.8 ± 2.3	P1 = 0.000	322.00 ± 11.6	8 ± 0.7	P2 = 0.000
P = 0.002, P between III and IV							
Type of granuloma	(10)			P = 0.000			P = 0.000
Absent	100%	(0) 0%	(0) 0%		(0) 0%	(0) 0%	
	0 (0%)	1 (20%)	5 (50%)		1 (20%)	2 (20%)	
Pregranulomatous/exudative Exudative/necrotic	0 (0%)	4 (80%)	4 (40%)		2 (40%)	0 (0%)	
Exudative/productive	0 (0%)	0 (0%)	1 (10%)		2 (40%)	8 (80%)	
Fibrosis	10						P = 0.025
Absent	(100%)				0 (0%)	2 (20%)	
Mild	0 (0%)				1 (20%)	8 (80%)	
Moderate	0 (0%)				4 (80%)	0 (0%)	

	Early phase				Late phase			
	GIIa	GIII			GIIb	GIV		
	Mean ± SD	Mean ± SD	% reduction	P value	Mean ± SD	Mean ± SD	% reduction	P value
No of hepatic granuloma (20 HPF)	21.8 ± 2.1	13 ± 0.9	40.63%	P < 0.001	24.4 ± 1	5.7 ± 0.2	76.63%	P < 0.001
Size of hepatic granuloma (10 HPF)	8698 ± 1186.8	4464.7 ± 502.2	48.66%	P = 0.108	8898 ± 1313	2929.1 ± 1489.6	67.08%	P = 0.008
No. of eosinophils (40 HPF)	320 ± 25.5	48.8 ± 2.3	84.75%	P < 0.001	322.00 ± 11.6	8 ± 0.7	97.5%	P < 0.001
Type of granuloma				P < 0.001				P < 0.001
Absent	(0) 0%	(0) 0%			(0) 0%	(0) 0%		
Exudative	1 (20%)	5 (50%)			1 (20%)	20 (100%)		
Exudative/necrotic	4 (80%)	4 (40%)			2 (40%)	0 (0%)		
Exudative/productive	0 (0%)	1 (10%)			2 (40%)	80 (80%)		
Fibrosis								P = 0.025
Absent					0 (0%)	2 (20%)		
Mild					1 (20%)	8 (80%)		
Moderate					4 (80%)	0 (0%)		

A T test was used to compare mean ± SD (standard deviation); the Monto-Carlo test was used to compare qualitative data. GIIa and GIIb: early and late positive control group (n=10); GIII: early-treated group infected mice with auranofin (n=20); GIV: late-treated group with praziquantel and auranofin (n=20)

and granulomatous inflammation are both down-regulated by reduced expression of IL-6 and IL-1β (pro-inflammatory cytokines) (Zhang *et al.* 2012). Blocking the NLRP3 inflammasome was the underlying mechanism and thus reduced the release of IL-1β and decreased the HSCs' capacity to migrate. Auranofin has an anti-inflammatory impact, and we hypothesized that inhibiting inflammasome activation would contribute to this effect and markedly decrease the region of granuloma and fibrosis in the liver in the current investigation.

Auranofin did not affect the NLRP3 inflammasome's priming signals. It only prevented caspase-1 from cleaving and IL-1β from maturing. Due to thioredoxin reductase modulation, previous studies have found increased levels of intracellular reactive oxygen species and decreased release of IL-1β by auranofin (Isakov *et al.* 2014; Lee *et al.* 2019). Similarly, Hwangbo *et al.* (2020) revealed that auranofin may have the potential to be a candidate for reducing the symptoms of non-alcoholic fatty liver disease by inhibiting the NLRP3 inflammasome (Hwangbo *et al.* 2020). Auranofin was also

https://doi.org/10.1017/S0022149X23000792 Published online by Cambridge University Press

Table 5. Comparative expression of IL-1β, SIRT3, and SMA during the early and late phases of infected and treated groups

	Early phase			Late phase		
	GIIa	GIII		GIIb	GIV	
	Mean ± SD	Mean ± SD	P value	Mean ± SD	Mean ± SD	P value
IL-1β expression	82.00 ± 4.89	36.00 ± 4.00	P < 0.001	94.00 ± 2.44	4.00 ± 0.745	P < 0.001
SIRT3	14.00 ± 2.91	112.00 ± 9.97	P < 0.001	13.00 ± 4.35	224.00 ± 5.61	P < 0.001
SMA portal tract and sinusoidal HSC			P < 0.001	83.00 ± 3.00	10.50 ± 1.38	P < 0.001

IL-1β: interleukin 1β, SIRT3: Sirtuin 3, SMA: Smooth muscle actin, HSC: Hepatic stellate cells. T test was used, mean ± SD (standard deviation). GIIa and GIIb: early and late positive control group (n=10); GIII: early-treated group infected mice with auranofin (n=20); GIV: late-treated group with auranofin (n=20)

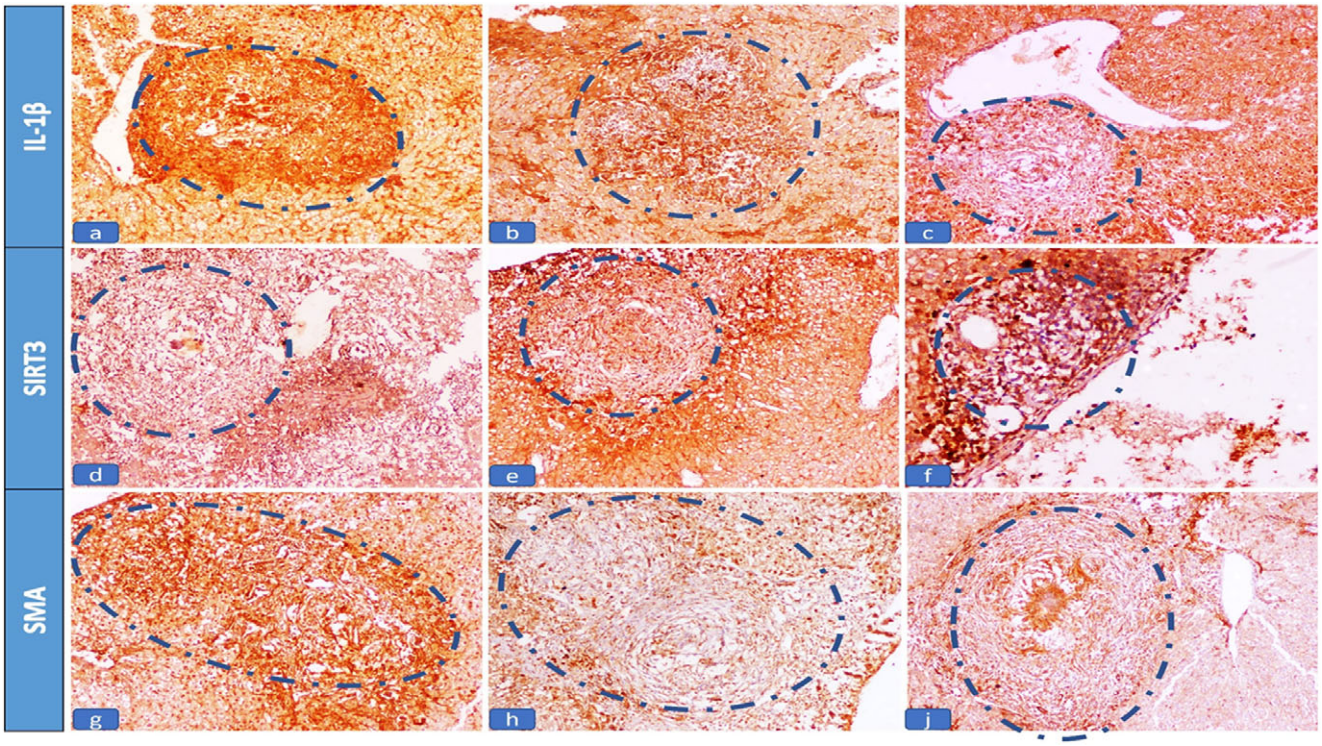

Figure 2. The immunohistochemical expression of IL-1β, SIRT3, and SMA in the studied groups. a) Mice infected untreated group (GIIa and GIIb) showed high IL-1β H score expression in the portal tracts (IHC, 100x), b) Mice early-treated group (GIII) showed moderate IL-1β H score expression in the portal tracts (IHC, 100x), c) Mice of late-treated group (GIV) showed low IL-1β H score expression in the portal tracts (IHC, 100x), d) Mice of infected untreated group (GIIa and GIIb) showed low SIRT3 H score expression in the portal tracts (IHC, 100x), e) Mice of early-treated group (GIII) showed moderate SIRT3 H score expression in the portal tracts (IHC, 100x), f) Mice of late-treated group (GIV) showed high SIRT3 H score expression in the portal tracts (IHC, 100x), g) Mice of infected untreated late group (GIIb) showed high SMA H score expression in the portal tracts (IHC, 100x), h) Mice of late-treated group (GIV) showed mild SMA H score expression in the portal tracts (IHC, 100x), j) Mice of late-treated group (GIV) showed mild SMA H score expression in the portal tracts (IHC, 100x).

shown by Kim *et al.* (2021) to considerably slow the progression of fibrosis in a thioacetamide- or carbon tetrachloride-induced fibrotic liver (Kim *et al.* 2021). Additionally, Kaufmann *et al.* (2022) found that the production of pro-inflammatory and pro-fibrotic cytokines as well as the onset of liver inflammation and fibrosis depends on the activation of the NLRP3 inflammasome complex in myeloid cells (Kaufmann *et al.* 2022). Production of cytokines, such as IL-1β, may occur after the activation of the NLRP3 inflammasome in KCs. In mice infected with *S. japonicum*, this activates HSCs and is accompanied by NLRP3 inflammasome activation, which is linked to the development of hepatic fibrosis (Zhang *et al.* 2019).

The present study showed that α-SMA expression in both portal tracts and sinusoidal HSC was significantly reduced in the auranofin late-treated group (GIV). Auranofin inhibits the migration of HSCs, which are the main suppliers of collagen and are essential for hepatic fibrogenesis. Quiescent HSCs are activated and transdifferentiated into myofibroblast-like cells under pathological circumstances; these cells express the myofibroblast marker and α-SMA and have increased collagen production (Xu *et al.* 2016). Consequently, one of the key features of HSC activation has been the development of α-SMA, which has grown in significance as a measure of hepatic fibrosis (Tsuchida and Friedman 2017).

Sirtuin 3 has beneficial effects on cellular responses and is sensitive to metabolic state (Liu *et al.* 2018). Here, we investigated how SIRT3-mediated autophagy affects NLRP3 inflammasome activity. The present study showed auranofin treatment causes a significantly higher expression of SIRT3. Similarly, Mukherjee *et al.*

https://doi.org/10.1017/S0022149X23000792 Published online by Cambridge University Press

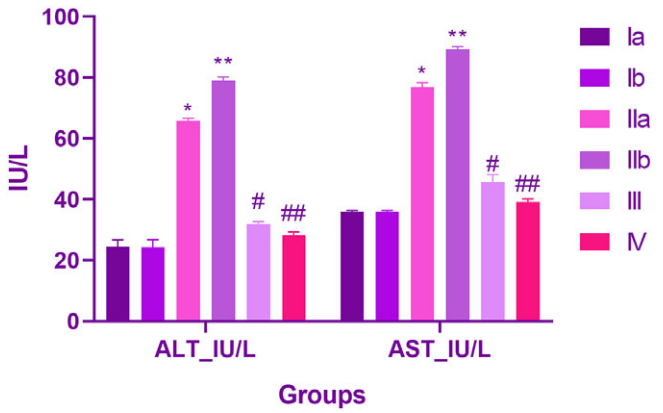

Figure 3. Alanine aminotransferase serum and aspartate aminotransferase serum levels IU/L (mean ± SD) in the different groups studied. GIa and GIb: early and late negative control group each (n=10); GIIa and GIIb: early and late positive control group each (n=10); GIII: early-treated group infected mice with auranofin (n=20); GIV: late-treated group auranofin (n=20).
ALT: alanine aminotransferase, AST: aspartate aminotransferase
*Mean values were significantly different from the GIa group: P < 0.05
**Mean values were significantly different from the GIb group: P < 0.05
#Mean values were significantly different from the GIIa group: P < 0.05
##Mean values were significantly different from the GIIb group: P < 0.05

(2021) established that the mitochondrial sirtuin, SIRT3, is crucial for liver regeneration (Mukherjee *et al.* 2021). SIRT3 may help prevent liver illnesses such as non-alcoholic fatty liver, liver damage, and fibrosis, according to mounting evidence (Xu *et al.* 2019). Similar results were obtained by Wang *et al.* (2020), who discovered that SIRT3 activation reduced liver fibrosis.

Loss of SIRT3 causes animals to be more sensitive to ischemia and other injuries (Lombard *et al.* 2007), and Sirtuin 3 has emerged as the main isoform responsible for reducing mitochondrial proteins (Zhang *et al.* 2020a). Furthermore, Zhang *et al.* (2020b) reported that AEDC (12βacetoxy-16,23-epoxy-24,25-dihydroxy3β-9,19-cyclolanost-22(23)-ene) inhibited the NLRP3 inflammasome through SIRT3-autophagy, which may be used to treat metabolic disorders linked to adipose tissue inflammation (Zhang *et al.* 2020b).

Autophagy-mediated NLRP3 inflammasome inhibition was concomitant with increases in SIRT3 levels (Liu *et al.* 2017), indicating that it might act as a mediator for auranofin's liver regeneration effects (Liu *et al.* 2018). Furthermore, Liu *et al.* (2017) demonstrated that SIRT3-deficient macrophages showed increased NLRP3 inflammasome activation, endothelial dysfunction, and defective autophagy (Liu *et al.* 2018). For the majority of liver cell types, autophagy is a cytoprotective and anti-fibrotic process, and it is essential for maintaining the metabolic homeostasis of hepatocytes (Khambu *et al.* 2018). Numerous disorders have been linked to the interaction between autophagy and the NLRP3 inflammasome, and the activation of this enzyme that causes pyroptosis has been linked to inflammation, fibrosis, and cell death in the liver (Al Mamun *et al.* 2020). Similarly, Wang *et al.* (2018) and Hao *et al.* (2022) demonstrated that lowering the levels of NLRP3, IL-1, IL-18, and caspase-1 improved hepatic dysfunction (Hao *et al.* 2022; Wang *et al.* 2018). The production of inflammasome-dependent IL-1β is inhibited by macrophage autophagy, which reduces acute toxin-induced liver injury and death in a mouse model (Ilyas *et al.* 2016). Alternatively, evidence indicates that autophagy plays a role in several anti-fibrotic processes that promote cell death and cell cycle arrest in HSCs or stop the production of pro-fibrotic mediators, such as excessive collagen accumulation (Lucantoni *et al.* 2021).

Conclusion

Auranofin prevents hepatic granulomas and fibrosis brought on by *S. mansoni* eggs. The NLRP3 inflammasome was blocked as a component of the underlying mechanism and thus decreased the release of IL-1β. Moreover, autophagy-mediated NLRP3 inflammasome inhibition was concomitant with an increase in SIRT3 levels that mediate the effect of auranofin on liver regeneration. Together with the restoration of serum ALT and AST towards normal levels, these findings reveal how auranofin suppresses the development of liver fibrosis. Therefore, it is important to reconsider auranofin as a potential therapy for hepatic granuloma and subsequent fibrosis induced by *S. mansoni* eggs.

Data availability statement. The data is available upon reasonable request to the corresponding author.

Author contribution. Amany Fawzy Atia, Noha Mohamed Abou-Hussein, Dina Mohamed Sweed, Eman Sweed, and Noha Ahmed Abo-khalil made major contributions to the work presented, whether in the conception, study design, execution, data gathering, analysis, or interpretation. Furthermore, Amany Fawzy Atia, Noha Mohamed Abou-Hussein, Dina Mohamed Sweed, Eman Sweed, and Noha Ahmed Abo-khalil contributed to the article's development and revision, agreed on the journal to which it will be submitted, and approved the final manuscript for publication. Finally, Amany Fawzy Atia, Noha Mohamed Abou-Hussein, Dina Mohamed Sweed, Eman Sweed, and Noha Ahmed Abo-khalil agreed to accept responsibility for all parts of the work, including ensuring that any doubts about the accuracy or integrity of any portion of the work are thoroughly explored.

Competing interest. No conflicts of interest were declared.

Ethics approval. The manuscript is exempt from the approval of the ethical committee.

References

Al Mamun A, Akter A, Hossain S, Sarker T, Safa SA, Mustafa QG, Muhammad SA, and Munir F (2020) Role of NLRP3 inflammasome in liver disease. *Journal of Digestive Diseases* **21**, 430–436. doi: 10.1111/1751-2980.12918

Alegre F, Pelegrin P, and Feldstein AE (2017) Inflammasomes in liver fibrosis. *Seminars in Liver Disease* **37**, 119–127. doi: 10.1055/s-0037-1601350

Amaral KB, Silva TP, Dias FF, Malta KK, Rosa FM, Costa-Neto SF, Gentile R, and Melo RC (2017) Histological assessment of granulomas in natural and experimental Schistosoma mansoni infections using whole slide imaging. *PLoS One* **12**, e0184696.

Andrade RM, Chaparro JD, Capparelli E, and Reed SL (2014) Auranofin is highly efficacious against Toxoplasma gondii in vitro and in an in vivo experimental model of acute toxoplasmosis. *PLOS Neglected Tropical Diseases* **8**, e2973. doi: 10.1371/journal.pntd.0002973

Angelucci F, Sayed AA, Williams DL, Boumis G, Brunori M, Dimastrogiovanni D, Miele AE, Pauly F, and Bellelli A (2009) Inhibition of Schistosoma mansoni thioredoxin-glutathione reductase by auranofin: structural and kinetic aspects. *Journal of Biological Chemistry* **284**, 28977–28985. doi: 10.1074/jbc.M109.020701

Bancroft J and Gamble M (2008) *Theory and practice of histology techniques*. London, Churchill Livingstone Elsevier, 83–134.

Bergmeyer H, Horder M, and Rej R (1986) Approved recommendation (1985) on IFCC methods for the measurement of catalytic concentration of enzymes. Part 2. IFCC method for aspartate aminotransferase (L-aspartate: 2-oxoglutarate aminotransferase, EC 2.6. 1.1). *Journal of Clinical Chemistry and Clinical Biochemistry* **24**, 497–508.

Cao Z, Wang Y, Long Z, and He G (2019) Interaction between autophagy and the NLRP3 inflammasome. *Acta Biochimica et Biophysica Sinica (Shanghai)* **51**, 1087–1095. doi: 10.1093/abbs/gmz098

Cheever AW (1969) Quantitative comparison of the intensity of Schistosoma mansoni infections in man and experimental animals. *Transactions of the Royal Society of Tropical Medicine and Hygiene* **63**, 781–795.

Chen S-Y, Chao C-N, Huang H-Y, and Fang C-Y (2022) Auranofin induces urothelial carcinoma cell death via reactive oxygen species production and synergy with cisplatin. *Oncology Letters* **23**, 61. doi: 10.3892/ol.2021.13179

Chen TTW, Cheng PC, Chang KC, Cao JP, Feng JL, Chen CC, Lam HP, and Peng SY (2019) Activation of the NLRP3 and AIM2 inflammasomes in a mouse model of Schistosoma mansoni infection. *Journal of Helminthology* **94**, e72. doi: 10.1017/s0022149x19000622

Chuah C, Jones MK, Burke ML, McManus DP, and Gobert GN (2014) Cellular and chemokine-mediated regulation in schistosome-induced hepatic pathology. *Trends in Parasitology* **30**, 141–150. doi: 10.1016/j.pt.2013.12.009

Debnath A, Ndao M, and Reed SL (2013) Reprofiled drug targets ancient protozoans. *Gut Microbes* **4**, 66–71. doi: 10.4161/gmic.22596

Ding Y, Fu X, Wang Q, Liu H, Wang H, and Wu D (2021) The complex interplay between autophagy and NLRP3 inflammasome in renal diseases. *International Journal of Molecular Sciences* **22**(23), 12766. doi: 10.3390/ijms222312766

El-Refai S, Atia A, and Mahmoud S (2019) Effects of Callistemon citrinus aqueous extract on prepatent and patent infections with Schistosoma mansoni in experimentally infected mice. *Journal of Helminthology*, **93**, 424–433.

Franchi L, Warner N, Viani K, and Nuñez G (2009) Function of Nod-like receptors in microbial recognition and host defense. *Immunological Reviews* **227**, 106–128. doi: 10.1111/j.1600-065X.2008.00734.x

Gaul S, Leszczynska A, Alegre F, Kaufmann B, Johnson CD, Adams LA, Wree A, Damm G, Seehofer D, and Calvente CJ (2021) Hepatocyte pyroptosis and release of inflammasome particles induce stellate cell activation and liver fibrosis. *Journal of Hepatology* **74**, 156–167.

Hao YY, Cui WW, Gao HL, Wang MY, Liu Y, Li CR, Hou L, and Jia ZH (2022) Jinlida granules ameliorate the high-fat-diet induced liver injury in mice by antagonising hepatocytes pyroptosis. *Pharmaceutical Biology* **60**, 274–281. doi: 10.1080/13880209.2022.2029501

He Z, Chen J, Zhu X, An S, Dong X, Yu J, Zhang S, Wu Y, Li G, and Zhang Y (2018) NLRP3 inflammasome activation mediates Zika virus–associated inflammation. *The Journal of Infectious Diseases* **217**, 1942–1951.

Hirschey MD, Shimazu T, Goetzman E, Jing E, Schwer B, Lombard DB, Grueter CA, Harris C, Biddinger S, Ilkayeva OR, Stevens RD, Li Y, Saha AK, Ruderman NB, Bain JR, Newgard CB, Farese Jr RV, Alt FW, Kahn CR, and Verdin E (2010) SIRT3 regulates mitochondrial fatty-acid oxidation by reversible enzyme deacetylation. *Nature* **464**, 121–125. doi: 10.1038/nature08778

Holanda J, Pellegrino J, and Gazzinelli G (1974) Infection of mice with cercariae and schistosomula of Schistosoma mansoni by intravenous and subcutaneous routes. *Revista do Instituto de Medicina Tropical de Sao Paulo* **16**, 132–134.

Hwangbo H, Kim MY, Ji SY, Kim SY, Lee H, Kim G-Y, Park C, Keum Y-S, Hong SH, and Cheong J (2020) Auranofin attenuates non-alcoholic fatty liver disease by suppressing lipid accumulation and NLRP3 inflammasome-mediated hepatic inflammation in vivo and in vitro. *Antioxidants* **9**, 1040.

Ilyas G, Zhao E, Liu K, Lin Y, Tesfa L, Tanaka KE, and Czaja MJ (2016) Macrophage autophagy limits acute toxic liver injury in mice through down regulation of interleukin-1β. *Journal of Hepatology* **64**, 118–127. doi: 10.1016/j.jhep.2015.08.019

Inzaugarat ME, Johnson CD, Holtmann TM, McGeough MD, Trautwein C, Papouchado BG, Schwabe R, Hoffman HM, Wree A, and Feldstein AE (2019) NLR family pyrin domain-containing 3 inflammasome activation in hepatic stellate cells induces liver fibrosis in mice. *Hepatology* **69**, 845–859. doi: 10.1002/hep.30252

Isakov E, Weisman-Shomer P, and Benhar M (2014) Suppression of the pro-inflammatory NLRP3/interleukin-1β pathway in macrophages by the thioredoxin reductase inhibitor auranofin. *Biochimica Et Biophysica Acta (BBA)-General Subjects* **1840**, 3153–3161.

Kaufmann B, Kui L, Reca A, Leszczynska A, Kim AD, Booshehri LM, Wree A, Friess H, Hartmann D, and Broderick L (2022) Cell-specific deletion of NLRP3 inflammasome identifies myeloid cells as key drivers of liver inflammation and fibrosis in murine steatohepatitis. *Cellular and Molecular Gastroenterology and Hepatology*, **14**, 751–767.

Khambu B, Yan S, Huda N, Liu G, and Yin X-M (2018) Homeostatic role of autophagy in hepatocytes. In *Seminars in Liver Disease*. vol. **38**. Thieme Medical Publishers, 308–319.

Kim HY, Choi YJ, Kim SK, Kim H, Jun DW, Yoon K, Kim N, Hwang J, Kim Y-M, and Lim SC (2021) Auranofin prevents liver fibrosis by system Xc-mediated inhibition of NLRP3 inflammasome. *Communications Biology* **4**, 824.

Kim HY, Kim KS, Kim MJ, Kim H-S, Lee K-Y, and Kang KW (2019) Auranofin inhibits RANKL-induced osteoclastogenesis by suppressing inhibitors of κB kinase and inflammasome-mediated interleukin-1β secretion. *Oxidative Medicine and Cellular Longevity*, 2019.

Kuntz AN, Davioud-Charvet E, Sayed AA, Califf LL, Dessolin J, Arnér ES, and Williams DL (2007) Thioredoxin glutathione reductase from Schistosoma mansoni: an essential parasite enzyme and a key drug target. *PLoS Medicine* **4**, e206. doi: 10.1371/journal.pmed.0040206

Lee D, Xu IMJ, Chiu DKC, Leibold J, Tse APW, Bao MHR, Yuen VWH, Chan CYK, Lai RKH, and Chin DWC (2019) Induction of oxidative stress through inhibition of thioredoxin reductase 1 is an effective therapeutic approach for hepatocellular carcinoma. *Hepatology* **69**, 1768–1786.

Lee H-M, Kim J-J, Kim HJ, Shong M, Ku BJ, and Jo E-K (2013) Upregulated NLRP3 inflammasome activation in patients with type 2 diabetes. *Diabetes* **62**, 194–204.

Lee HY, Kim J, Quan W, Lee JC, Kim MS, Kim SH, Bae JW, Hur KY, and Lee MS (2016) Autophagy deficiency in myeloid cells increases susceptibility to obesity-induced diabetes and experimental colitis. *Autophagy* **12**, 1390–1403. doi: 10.1080/15548627.2016.1184799

Levine B and Deretic V (2007) Unveiling the roles of autophagy in innate and adaptive immunity. *Nature Reviews Immunology* **7**, 767–777. doi: 10.1038/nri2161

Liang Y, Bruce J, and Boyd D (1987) Laboratory cultivation of schistosome vector snails and maintenance of schistosome life cycles. In *Proceeding of the 1st Sino-American Symposium*, vol. **1**, 34–48.

Liu P, Huang G, Wei T, Gao J, Huang C, Sun M, Zhu L, and Shen W (2018) Sirtuin 3-induced macrophage autophagy in regulating NLRP3 inflammasome activation. *Biochimica et Biophysica Acta (BBA)-Molecular Basis of Disease* **1864**, 764–777.

Lombard DB, Alt FW, Cheng HL, Bunkenborg J, Streeper RS, Mostoslavsky R, Kim J, Yancopoulos G, Valenzuela D, Murphy A, Yang Y, Chen Y, Hirschey MD, Bronson RT, Haigis M, Guarente LP, Farese Jr RV, Weissman S, Verdin E, and Schwer B (2007) Mammalian Sir2 homolog SIRT3 regulates global mitochondrial lysine acetylation. *Molecular and Cellular Biology* **27**, 8807–8814. doi: 10.1128/mcb.01636-07

Lu A and Wu H (2015) Structural mechanisms of inflammasome assembly. *Febs* **282**, 435–444. doi: 10.1111/febs.13133

Lucantoni F, Martínez-Cerezuela A, Gruevska A, Moragrega Á B, Víctor VM, Esplugues JV, Blas-García A, and Apostolova N (2021) Understanding the implication of autophagy in the activation of hepatic stellate cells in liver fibrosis: are we there yet? *Journal of Pathology* **254**, 216–228. doi: 10.1002/path.5678

Mahla R, Reddy C, Prasad D, and Kumar H (2013) Sweeten PAMPs: role of sugar complexed PAMPs in innate immunity and vaccine biology. *Frontiers in Immunology* **4**. doi: 10.3389/fimmu.2013.00248

Mao L, Zhang L, Li H, Chen W, Wang H, Wu S, Guo C, Lu A, Yang G, and An L (2014) Pathogenic fungus Microsporum canis activates the NLRP3 inflammasome. *Infection and Immunity* **82**, 882–892.

Meng N, Xia M, Lu YQ, Wang M, Boini KM, Li PL, and Tang WX (2016) Activation of NLRP3 inflammasomes in mouse hepatic stellate cells during *Schistosoma J. infection*. Oncotarget **7**, 39316–39331. doi: 10.18632/oncotarget.10044

Mohamed AH, El-Din ATS, Mohamed AM, and Habib MR (2011) Tissue responses exhibited by Biomphalaria alexandrina snails from different Egyptian localities following Schistosoma mansoni exposure. *Experimental Parasitology* **127**, 789–794.

Mukherjee S, Mo J, Paolella LM, Perry CE, Toth J, Hugo MM, Chu Q, Tong Q, Chellappa K, and Baur JA (2021) SIRT3 is required for liver regeneration but not for the beneficial effect of nicotinamide riboside. *JCI Insight*, **6**, 147193.

Nagy LE (2015) The role of innate immunity in alcoholic liver disease. *Alcohol Research* **37**, 237–250.

https://doi.org/10.1017/S0022149X23000792 Published online by Cambridge University Press

Ning ZW, **Luo XY**, **Wang GZ**, **Li Y**, **Pan MX**, **Yang RQ**, **Ling XG**, **Huang S**, **Ma XX**, **Jin SY**, **Wang D, and Li X** (2017) MicroRNA-21 mediates Angiotensin II-induced liver fibrosis by activating NLRP3 inflammasome/IL-1β axis via targeting Smad7 and Spry1. *Antioxidants & Redox Signaling* **27**, 1–20. doi: 10.1089/ars.2016.6669

Niu X, **Hu T**, **Hong Y**, **Li X, and Shen Y** (2022) The role of praziquantel in the prevention and treatment of fibrosis associated with schistosomiasis: a review. *Journal of Tropical Medicine* **2022**, 1413711. doi: 10.1155/2022/1413711

Pellegrino J, **Oliveira CA**, **Faria J, and Cunha AS** (1962) New approach to the screening of drugs in experimental schistosomiasis mansoni in mice. *American Journal of Tropical Medicine and Hygiene* **11**, 201–215.

Percie du Sert N, **Hurst V**, **Ahluwalia A**, **Alam S**, **Avey MT**, **Baker M**, **Browne WJ**, **Clark A**, **Cuthill IC**, **Dirnagl U**, **Emerson M**, **Garner P**, **Holgate ST**, **Howells DW**, **Karp NA**, **Lazic SE**, **Lidster K**, **MacCallum CJ**, **Macleod M**, **Pearl EJ**, **Petersen OH**, **Rawle F**, **Reynolds P**, **Rooney K**, **Sena ES**, **Silberberg SD**, **Steckler T, and Würbel H** (2020) The ARRIVE guidelines 2.0: updated guidelines for reporting animal research. *British Journal of Pharmacology* **177**, 3617–3624. doi: 10.1111/bph.15193

Pu X, **Storr SJ**, **Zhang Y**, **Rakha EA**, **Green AR**, **Ellis IO, and Martin SG** (2017) Caspase-3 and caspase-8 expression in breast cancer: caspase-3 is associated with survival. *Apoptosis* **22**, 357–368.

Seki E and Schwabe RF (2015) Hepatic inflammation and fibrosis: functional links and key pathways. *Hepatology* **61**, 1066–1079.

Steers GJ, **Chen GY**, **O'Leary BR**, **Du J**, **Van Beek H, and Cullen JJ** (2022) Auranofin and pharmacologic ascorbate as radiomodulators in the treatment of pancreatic cancer. *Antioxidants* **11**, 971.

Tendler M, **Pinto RM**, **Lima AO**, **Gebara G, and Katz N** (1986) Schistosoma mansoni: vaccination with adult worm antigens. *International Journal for Parasitology* **16**, 347–352.

Tsuchida T and Friedman SL (2017) Mechanisms of hepatic stellate cell activation. *Nature Reviews Gastroenterology & Hepatology* **14**, 397–411.

Vakrakou AG, **Boiu S**, **Ziakas PD**, **Xingi E**, **Boleti H, and Manoussakis MN** (2018) Systemic activation of NLRP3 inflammasome in patients with severe primary Sjögren's syndrome fueled by inflammagenic DNA accumulations. *Journal of Autoimmunity* **91**, 23–33.

Van de Vijver KK, Colpaert CG, **Jacobs W**, **Kuypers K**, **Hokke CH**, **Deelder AM, and Van Marck EA** (2006) The host's genetic background determines the extent of angiogenesis induced by schistosome egg antigens. *Acta Tropica* **99**, 243251. doi: 10.1016/j.actatropica.2006.08.011

Wang J, **Ren H**, **Yuan X**, **Ma H**, **Shi X, and Ding Y** (2018) Interleukin-10 secreted by mesenchymal stem cells attenuates acute liver failure through inhibiting pyroptosis. *Hepatology Research* **48**, e194–e202. doi: 10.1111/hepr.12969

Wang Y, **Li C**, **Gu J**, **Chen C**, **Duanmu J**, **Miao J**, **Yao W**, **Tao J**, **Tu M**, **Xiong B**, **Zhao L, and Liu Z** (2020) Celastrol exerts anti-inflammatory effect in liver fibrosis via activation of AMPK-SIRT3 signalling. *Journal of Cellular and Molecular Medicine* **24**, 941–953. doi: 10.1111/jcmm.14805

WHO (2022) Schistosomiasis *Secondary Schistosomiasis* https://www.who.int/health-topic/schistosomiasis (accessed 24 January 2023).

Wree A, **McGeough MD**, **Inzaugarat ME**, **Eguchi A**, **Schuster S**, **Johnson CD**, **Peña CA**, **Geisler LJ**, **Papouchado BG**, **Hoffman HM, and Feldstein AE** (2018) NLRP3 inflammasome driven liver injury and fibrosis: roles of IL-17 and TNF in mice. *Hepatology* **67**, 736—49. doi: 10.1002/hep.29523

Wree A, **McGeough MD**, **Peña CA**, **Schlattjan M**, **Li H**, **Inzaugarat ME**, **Messer K**, **Canbay A**, **Hoffman HM, and Feldstein AE** (2014) NLRP3 inflammasome activation is required for fibrosis development in NAFLD. *Journal of Molecular Medicine* **92**, 1069–1082. doi: 10.1007/s00109-014-1170-1

Xu H, **Hertzel AV**, **Steen KA, and Bernlohr DA** (2016) Loss of fatty acid binding protein 4/aP2 reduces macrophage inflammation through activation of SIRT3. *Molecular Endocrinology* **30**, 325–334. doi: 10.1210/me.2015-1301

Xu X, **Zhu XP**, **Bai JY**, **Xia P**, **Li Y**, **Lu Y**, **Li XY, and Gao X** (2019) Berberine alleviates nonalcoholic fatty liver induced by a high-fat diet in mice by activating SIRT3. *Faseb Journal* **33**, 7289–7300. doi: 10.1096/fj.201802316R

Zhang J, **Xiang H**, **Liu J**, **Chen Y**, **He RR, and Liu B** (2020a) Mitochondrial Sirtuin 3: new emerging biological function and therapeutic target. *Theranostics* **10**, 8315–8342. doi: 10.7150/thno.45922

Zhang T, **Fang Z**, **Linghu KG**, **Liu J**, **Gan L, and Lin L** (2020b) Small molecule-driven SIRT3-autophagy-mediated NLRP3 inflammasome inhibition ameliorates inflammatory crosstalk between macrophages and adipocytes. *British Journal of Pharmacology* **177**, 4645–4665. doi: 10.1111/bph.15215

Zhang W-J, **Fang Z-M, and Liu W-Q** (2019) NLRP3 inflammasome activation from Kupffer cells is involved in liver fibrosis of Schistosoma japonicum-infected mice via NF-κB. *Parasites & Vectors* **12**, 29. doi: 10.1186/s13071-018-3223-8

Zhang Y, **Chen L**, **Gao W**, **Hou X**, **Gu Y**, **Gui L**, **Huang D**, **Liu M**, **Ren C, and Wang S** (2012) IL-17 neutralization significantly ameliorates hepatic granulomatous inflammation and liver damage in S chistosoma japonicum infected mice. *European Journal of Immunology* **42**, 1523–1535.

https://doi.org/10.1017/S0022149X23000792 Published online by Cambridge University Press